Hindawi
Shock and Vibration
Volume 2021, Article ID 7227194, 14 pages
https://doi.org/10.1155/2021/7227194

Research Article

Experimental Study on the Evolution of Argillization of Mudstone and Cutter Wear during the TBM Tunnelling

Kanglei Song, Bolong Liu, and Haiqing Yang

School of Civil Engineering, Chongqing University, Chongqing 400045, China

Correspondence should be addressed to Bolong Liu; 20171601009@cqu.edu.cn

Received 7 August 2021; Revised 15 September 2021; Accepted 9 October 2021; Published 22 October 2021

Academic Editor: Bin Gong

Argillization is a process in which clay-bearing rocks disintegrate into the clay under the action of high temperature, pressure, and water. When tunnel boring machines (TBMs) excavate in the mudstone, argillization takes place, causing the clogging of the TBM cutterhead. As a result, the penetration rate drops gradually. Abnormal wear might occur. To investigate the evolution of argillization of mudstone and cutter wear during the TBM tunnelling, a series of rotary indentation tests were carried out on the self-designed experimental bench for different loading times. During the test, the temperature and penetration depth of disc cutters were measured in real time. After loading, microstructures of cutting grooves, slacking mudstone, and worn cutter ring were observed by stereomicroscope. Consequently, the evolution of argillization in mudstone and cutter wear were investigated. Experimental results indicate that the argillization process of mudstone by disc cutter can be divided into three stages: mechanical cutting stage, deterioration of mudstone and the formation of slacking mudstone stage, and adherence of slacking mudstone stage. Specifically, at mechanical cutting stage, the rock was cut by cutter directly, causing high frictional heat. Then the microstructure of mudstone was deteriorated due to the water-weakening mechanisms, temperature effect, and mechanical activation effect. Finally, the slacking mudstone was adhered to the disc cutter. Correspondingly, due to the argillization of mudstone, the disc cutter wear goes through the mechanical wear stage, argillization wear stage, and secondary wear stage in sequence. This investigation reveals the rock cutting mechanism of TBM considering the argillization of mudstone. Furthermore, it provides some references for design and operation of the TBM.

1. Introduction

The TBM is commonly employed in the mechanized excavation of tunnels [1]. During TBM tunnelling, owning to the mechanical operation and friction between cutter and rock, frictional heat is generated. In particular, when the TBMs excavate in the mudstone stratum, the mudstone will transform into the mud under the action of high temperature, cutter pressure, and water. This process can be defined as the argillization of mudstone. A large amount of mud will be adhered to the cutter and cutterhead, causing the "mud cake" and the clogging of TBMs [2–4]. The phenomenon could also cause the flat wear of disc cutters; thus the wear loss will increase dramatically. Frequent cutter replacement leads to time delay and budget overruns, which seriously affects the TBM construction progress. Consequently, it is of high significance to investigate the argillization of mudstone by disc cutter and cutter wear under the condition of argillization.

Due to the complexity of geological conditions, adverse stratums are frequently encountered during the TBM excavation. Therefore, many works have focused on the rock fragmentation mechanism in various conditions, such as the intact rock, jointed rock mass, and mixed face ground [5–8]. The rock fragmentation mechanism by disc cutter differs from that by other tools [9–11]. When the disc cutter penetrates into intact rock, a crushed zone is firstly formed under the compression of cutter tips. As loading progresses, the minor crack and major cracks propagate from the crushed zone. Once the cracks between disc cutters coalescence with each other or reach to the free surface, the rock chips are formed [12]. However, in the jointed rock mass, the

cracking process by disc cutter exerts different features. Joint spacing and joint orientation are main factors influencing rock fragmentation. In detail, Liu et al. [13] conducted a serious two-dimensional indentation test on jointed rock with different orientations. The experimental results reveal that joint orientation will change the relative magnitude of tensile and shear stresses along the trajectory of median cracks. The rock fragmentation modes for different joint orientations can be divided into rock breakage by individual cutter (0 deg), rock breakage by synergetic effects of cutters and joint plants (30–60 deg), and rock breakage by synergetic effects of cutters (90 deg). The cutting efficiency reaches the maximum value at the orientation of 60 deg. Gong et al. [14] investigated the effect of joint spacing on rock breaking in the Jinping Hydropower Project. According to the field investigation, it was found that big rock chips were usually formed in the rock mass with thin layer, which means the high rock cutting efficiency of TBM. In the mixed face ground, the rock fragmentation process will become more complex. Owing to the difference of physical and mechanical properties between soft and hard rock, abnormal cutter wear, face instability, muck transportation problems, and ground settlement are usually encountered during the TBM tunnelling [15–18]. However, the research on the rock cutting mechanism in the clay-bearing rock is rarely reported. In particular, when the TBMs excavate in mudstone, the argillization mechanism is unclear.

During the tunnelling, another important consideration for TBMs is cutter wear. The wear mechanism has been one of the major subjects in both academic field and engineering field. To date, it has been acknowledged that the wear mechanism of disc cutter is classified as tribochemical reaction, surface fatigue, adhesive wear, and abrasive wear [19]. Among them, abrasive wear is the most common wear form [20]. Ploughing, microcutting, microfatigue, and microcracking are main reasons for the abrasive wear [21, 22]. When disc cutters roll on the tunnel face, wear loss is affected by many factors, such as properties of cutter, geological conditions, and operational conditions [23, 24]. For example, on the basic of Cerchar test, Michalakopoulos et al. [25] investigated the effect of steel hardness on Cerchar Abrasivity Index (CAI), which represents the abrasiveness of rocks. Afterwards, Macias et al. [26] developed a novel test named Rolling Indentation Abrasion Test (RIAT) to simulate the cutter wear process in a realistic way. In this study, the influences of rock types, CAI, Abrasion Value cutter Steel (AVS), and mineral compositions on wear loss were investigated. Considering that dry rock grounds, moist rock grounds, or seawater might be encountered during the tunnelling, Zhang et al. [27] investigated the wear behaviors of disc cutter under drying, water, and seawater conditions through linear cutter test. By comparison, it was found that the water reduces the mass loss due to the lubricant effect, while the seawater corrodes the cutter, leading to the aggravation of wear. For the jointed rock mass and the mixed face ground, Liu et al. [28] experimentally studied the influences of jointed orientation and the strength of interlayer on the disc cutter wear. It was found that the cutter wear reaches the minimum value at the jointed orientation of 30 deg. The increase of the strength of soft interlayers is helpful for decreasing wear loss. Besides, the cutter wear for different cutterhead thrusts and rotational speeds was also studied. Regrettably, on consideration of the argillization of mudstone, the evolution of the cutter wear is still unclear.

In the present study, to investigate the argillization of mudstone and cutter wear mechanism during the TBM tunnelling, a series of rotary indentation tests were carried out on the self-design experimental bench. The microstructures of cutting grooves, slacking mudstone, and disc cutter for different penetration times were observed by stereo microscope. Besides, the temperature on disc cutter and the wear loss of cutter were measured. According to the results, the argillization of mudstone and cutter wear during the TBM tunnelling is divided into three stages; the mechanism at each stage is revealed.

2. Experimental Design

2.1. Preparation of Rock Samples. The mudstone taken from Chongqing was selected as rock samples in the experiment. Given the size of the test bench in this experiment, the mudstone sample is cut into a cube with dimension of 100 mm × 80 mm × 80 mm. The flatness of the surface of the sample is less than 1 mm, as shown in Figure 1. The physical and mechanical properties of the mudstone samples are listed in Table 1.

To investigate the evolution of the argillization in mudstone and cutter wear, rock blocks were classified into 8 groups of each of these 3 rocks. In the experiment, it was found that the penetration depth increases rapidly before the loading time of 20 min. Subsequently, the growth rate slows down. Thus, to investigate the evolution of argillization of mudstone and cutter wear accurately, the penetration time of each group is set as 5 min, 10 min, 15 min, 20 min, 30 min, 40 min, 50 min, and 60 min, respectively.

2.2. Experimental Instrument and Process. In the rotary indentation test, a self-designed test bench was employed, as illustrated in Figure 2(a). The test bench mainly consists of an electromotor, steel support, slide rails, a pair of weights, and a reduced disc cutter. In detail, the size of the test bench is 570 mm in length, 300 mm in width, and 300 mm in height. The reduced disc cutter installed on the drive shaft is driven by the electromotor. At the same time, the rock block slides downward along the rails under the action of weights. As a result, disc cutter penetrates into the mudstone rock block. The reduced disc cutter with diameter of 70 mm represents the 17-inch cutter (432 mm) in the engineering practice (Figure 2(b)). Therefore, the reduced scale is 1: 6.17. The reduced cutter is made of H13 steel with Rockwell hardness HRC of 45 ± 1. In addition, D384 M infrared camera was used to measure the temperature on the cutter in a real time. The microstructures of rock blocks and disc cutters can be observed by OLYMPUS SZX16 stereo microscope. The infrared camera has a resolution of 384 × 288 pixels, a measurement range of −20°C to 150°C, and a thermal sensitivity of 0.04°C.

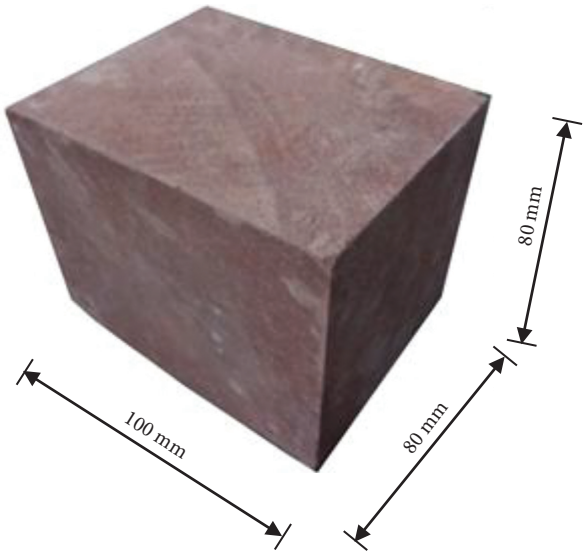

Figure 1: The size of mudstone specimen.

Table 1: The physical and mechanical properties of mudstone.

Parameters	Value
Destiny (g/cm^3)	2.65
Elastic modulus (MPa)	1820
Uniaxial compressive strength (MPa)	8.65
Brazilian tensile strength (MPa)	1.32
Poisson's ratio	0.23
Cohesion (MPa)	0.68
Internal friction angle (°)	32.2

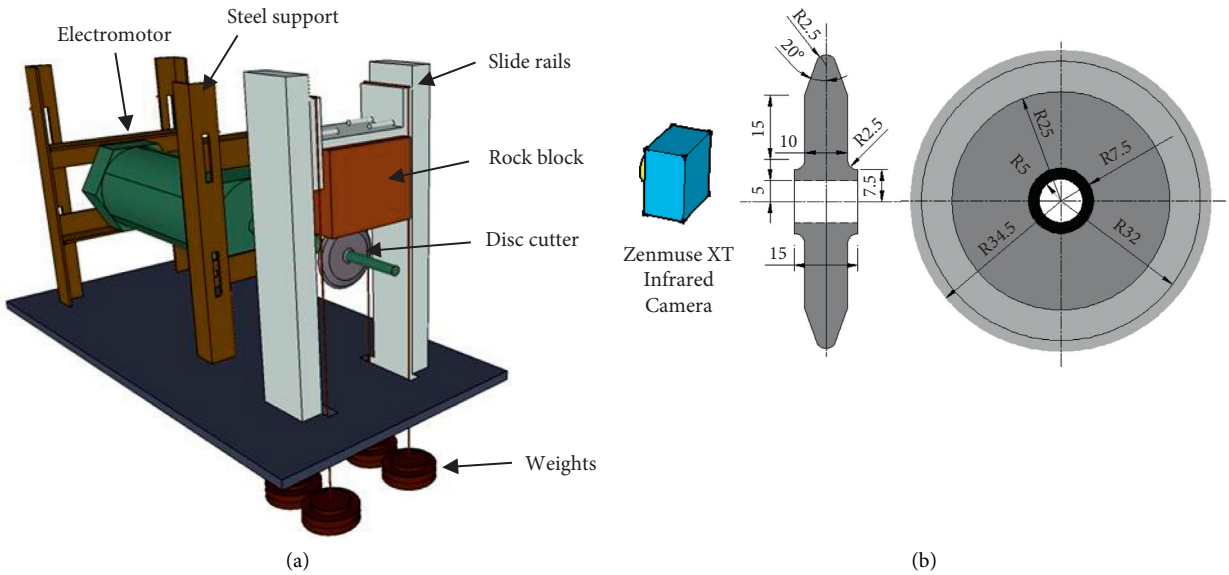

Figure 2: Schematic diagram of cutter rotary indentation tests. (a) Test bench; (b) the size of reduced scale disc cutter.

Before the loading, the rock block was installed on the slide rails. The infrared camera was placed 0.5 m away from the rock. After that, turning on the electromotor and the infrared thermal imager at the same time, the test begins. During the loading process, the temperature on the cutter and the displacement of the rock block were measured by infrared camera and displacement meter at interval of 5 minutes, respectively. Thus, the indentation

depth can be obtained. During the tunnelling, the rock powders, i.e., slaking mudstone, were collected in a real time, which were generated due to the rotation of disc cutter. To simulate the watering of cutterhead in TBM, water was sprayed randomly on the disc cutter during the experiment. The water addition is 0.6 g/min. According to the engineering experience, the average linear velocity of disc cutter varies from 0.8 m/s to 1.7 m/s. Therefore, the rotational speed of the cutter was set as 70 rpm. Generally, Abrasion Value cutter Steel (AVS) test and Sievers's J value test [5] are employed to evaluate the rock abrasivity. In these tests, mass of weight is 10 kg and 15 kg, respectively. Thus, the mass of weights in the present experiment was adopted as 15 kg. After the experiment, stereo microscope was employed to observe the microstructures of the rock cutting groove, slacking mudstone, and the worn surface of disc cutter. In addition, the mass of the cutter before and after the loading was weighted. Three repeated tests were conducted for each group.

It should be noticed that the motion mode of the disc cutter in this experiment differs from that in engineering practice. The cutter revolves around drive shaft instead of rolling on the rock. The friction between disc cutter and the rock is obvious. Hertz elastic contact theory has pointed out that slip also occurs in the contact area between disc cutter and the rock when the cutter rolls [29]. In this study, the main purpose is to investigate the argillization of mudstone. Thus, the motion mode of the disc cutter in this experiment will make the argillization more obvious.

3. Experimental Results

In the experiment, microstructures of cutting groove, slaking mudstone, and worn surface of disc cutter wear were observed at 400 magnification. According to the photomicrographs, the porosity of cutting groove and average particle size of slaking mudstone were obtained by the image processing software ImageJ. Besides, the curves of wear loss at different penetration depths were plotted.

3.1. Microstructures of Cutting Groove and Slaking Mudstone during the TBM Tunnelling. The photomicrographs of cutting groove and slaking mudstone at different penetration depths are shown in Figures 3 and 4, respectively. In the figures, P/D represents the ratio of the penetration depth P of the cutter to the diameter of cutter D. The experimental results indicate that when the loading time is 5 min ($P/D = 0.04$), microcracks and abrasion mark occur on the cutting groove (Figure 3(a)). In addition to loose particles, a small amount of flaky aggregates is found in the slaking mudstone (Figure 4(a)). Later, as the time increases to 10–20 min, the microcrack and abrasion mark disappear, while some micropores appear on the surface of the cutting groove. Besides, slacking mudstone gradually occurs; thus the surface of cutting grooves becomes relatively flat as shown in Figures 3(b)–3(d). Accordingly, at this stage, the slaking mudstone becomes agglomerate. A small number of micropores can be seen on the surface as shown in Figures 4(b)–4(d). When the loading time exceeds 30 min, the slaking mudstone on the cutting groove surface disappears, leaving some micropits and micropores. The skeletal particles are obvious (Figures 3(e)–3(h)). In this case, the slacking mudstone expands and becomes looser than those at loading time of 10–20 min (Figures 4(e)–4(h)).

To quantitatively analyze the characteristics of the cutting groove and the microstructure of the slaking mudstone, the porosity and average particle size in Figures 3 and 4 are further measured by the image processing software ImageJ, respectively. In ImageJ, the photomicrographs of cutting grooves were firstly transformed into grayscale images. By setting an appropriate threshold, all the micropores in the picture show as black spot. The area ratio of black spot to the whole picture is the porosity. Besides, on the bases of reduced scale, the dimeter of each particle in the pictures was measured. Thus the average particle size of the slaking mudstone in the picture was obtained. The results are plotted in Figure 5. In this figure, it is shown that the porosity of the cutting groove gradually decreases from 10.95% to 4.42% when $P/D \leq 0.09$ (5–20 min). After $P/D \geq 0.13$ (30–60 min), the value increases (Figure 5(a)). However, the inverse trend is seen for the average particle size of slacking mudstone. Specifically, the value increases when $P/D \leq 0.09$ (5–20 min). At P/D of 0.09, it reaches the peak point (251.47 μm). In addition, the variance of particle size is also greater than that at other moments when $P/D = 0.09$, indicating that the particle size distribution is not uniform at this time.

3.2. Cutter Wear Process during the TBM Tunnelling. The variation of cutter wear per revolution is plotted in Figure 6. In this figure, cutter wear represents the average wear loss per revolution during the loading times of 0–5 min, 5–10 min, 10–15 min, 15–20 min, 20–30 min, 30–40 min, 40–50 min, and 50–60 min. At the loading times of 0–5 min ($P/D < 0.06$), the cutter wear is 0.06 mg/r. After that, the value becomes decreased, and the minimum value is 0.025 mg/r ($P/D = 0.06$). However, when the time exceeds 15 min, cutter wear increases dramatically. The maximum value reaches 0.19 mg/r ($P/D = 0.18$), which is 1.27 times larger than the minimum value.

The microstructures of the worn surface of cutter were observed, as illustrated in Figure 7. At loading time of 5 min, ($P/D = 0.04$), microcutting is obviously observed on the cutter surface. In addition, some loose and flaky particles are found as shown in Figure 7(a). At the duration of 10–20 min ($0.06 \leq P/D \leq 0.09$), microcutting disappears gradually. Instead, much slacking mudstone adheres to the disc cutter as shown in Figures 7(b)–7(d). With the loading processes, microcutting can be observed again as shown in Figures 7(e)–7(g). Eventually, the worn surface of disc cutter is covered by slacking mudstone as shown in Figure 7(h).

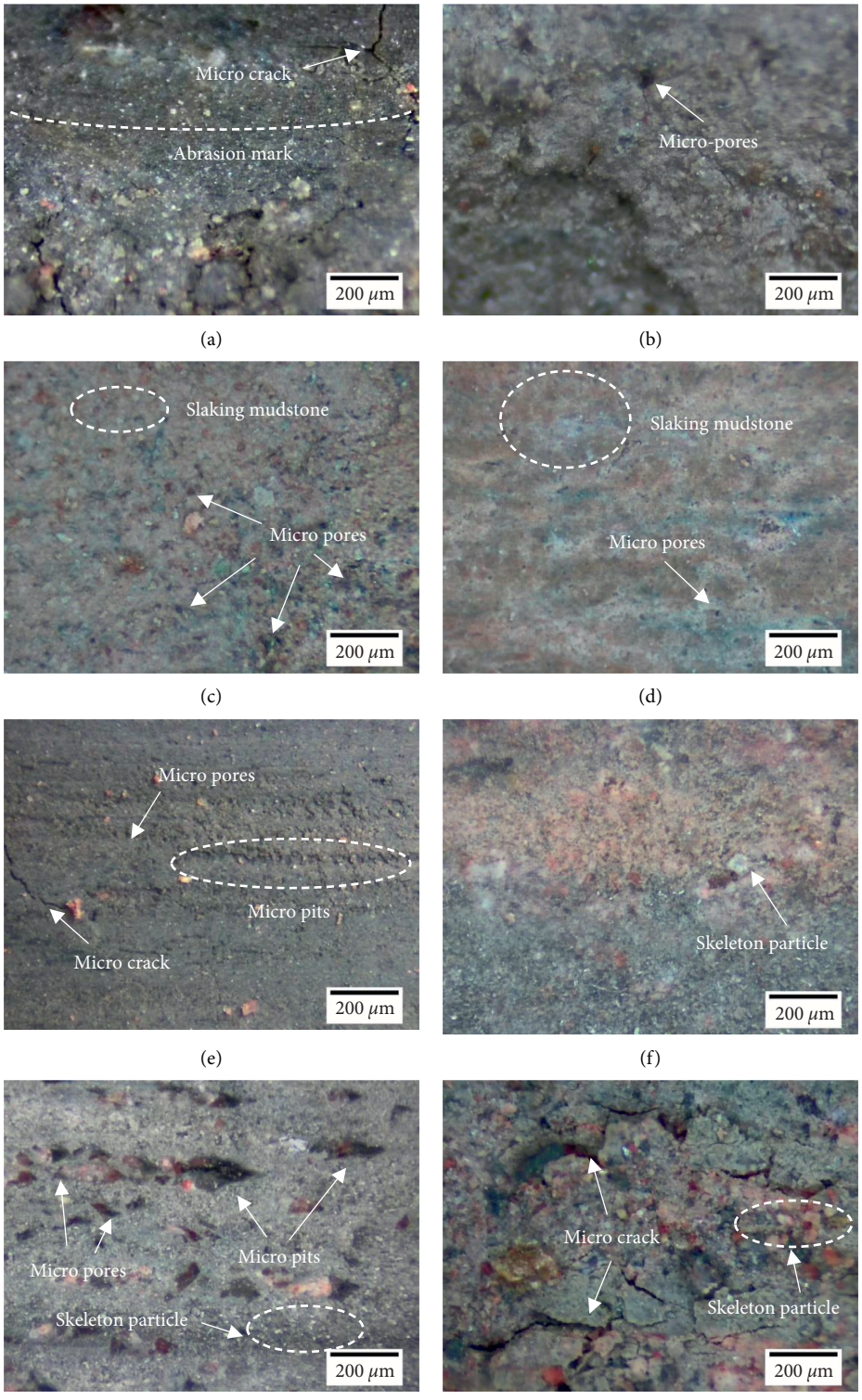

Figure 3: Evolution of microstructures of cutting grooves of rock blocks at ×400 magnification. (a) 5 min, $P/D = 0.04$; (b) 10 min, $P/D = 0.06$; (c) 15 min, $P/D = 0.07$; (d) 20 min, $P/D = 0.09$; (e) 30 min, $P/D = 0.13$; (f) 40 min, $P/D = 0.15$; (g) 50 min, $P/D = 0.17$; (h) 60 min, $P/D = 0.18$.

4. Discussions

In this section, based on the microstructure of cutting grooves, slacking mudstone, and disc cutter for different loading times, the evolution of argillization of mudstone and cutter wear mechanism during the TBM tunnelling are analyzed. Specifically, the argillization of mudstone is divided into mechanical cutting stage, the deterioration of mudstone and the formation

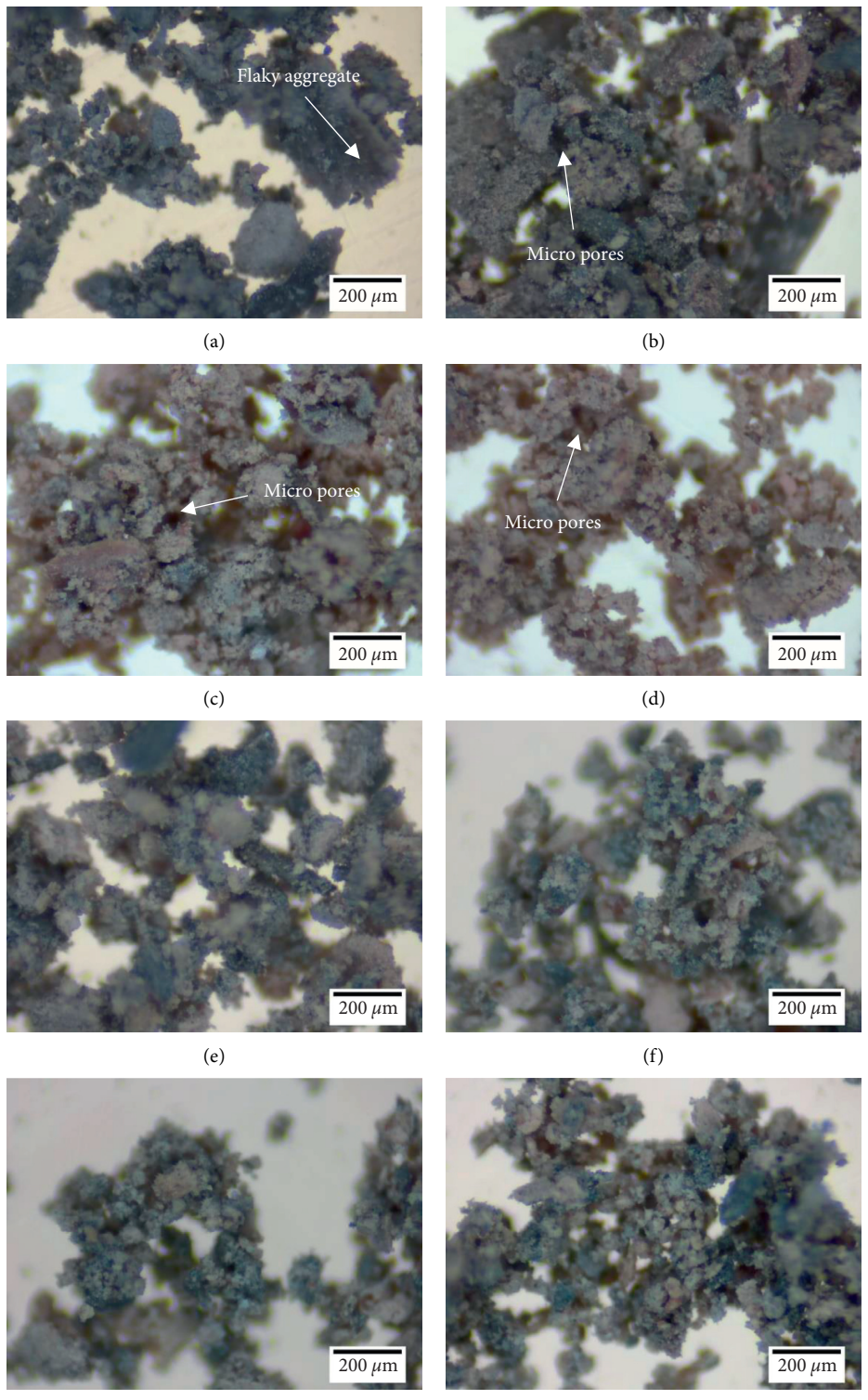

Figure 4: Evolution of microstructure of slaking mudstone at ×400 magnification. (a) 5 min, $P/D = 0.04$; (b) 10 min, $P/D = 0.06$; (c) 15 min, $P/D = 0.07$; (d) 20 min, $P/D = 0.09$; (e) 30 min, $P/D = 0.13$; (f) 40 min, $P/D = 0.15$; (g) 50 min, $P/D = 0.17$; (h) 60 min, $P/D = 0.18$.

of slacking mudstone stage, and adhesion of slacking mudstone stage. Correspondingly, due to the argillization in mudstone, the disc cutter wear goes through the mechanical wear stage, argillization wear stage, and secondary wear stage. The mechanisms of argillization and cutter wear considering argillization at each stage are revealed.

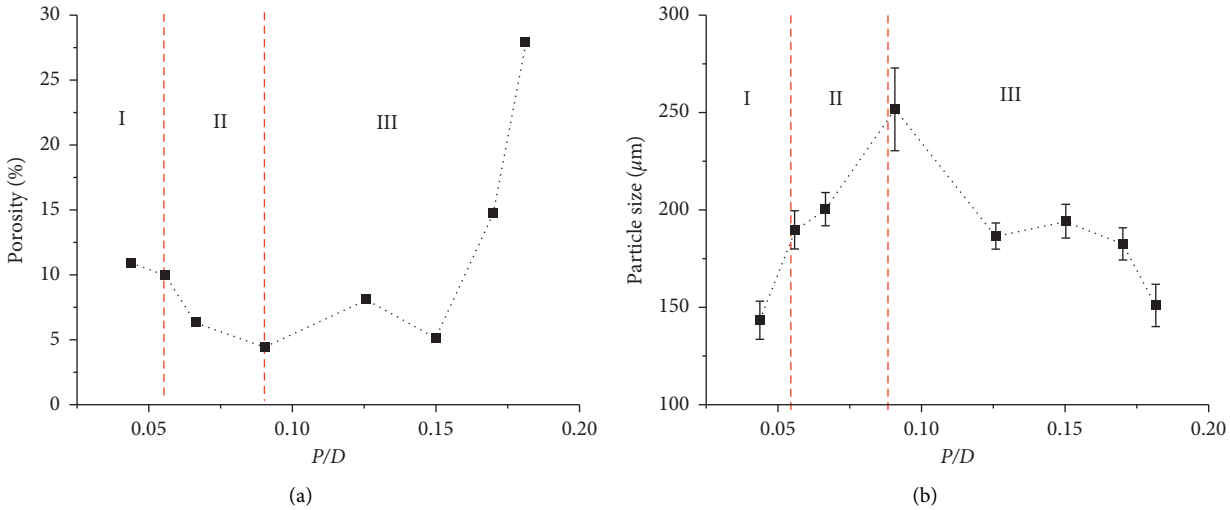

Figure 5: Variations of the (a) porosity of cutting groove of rock blocks and (b) particle size of slaking mudstone.

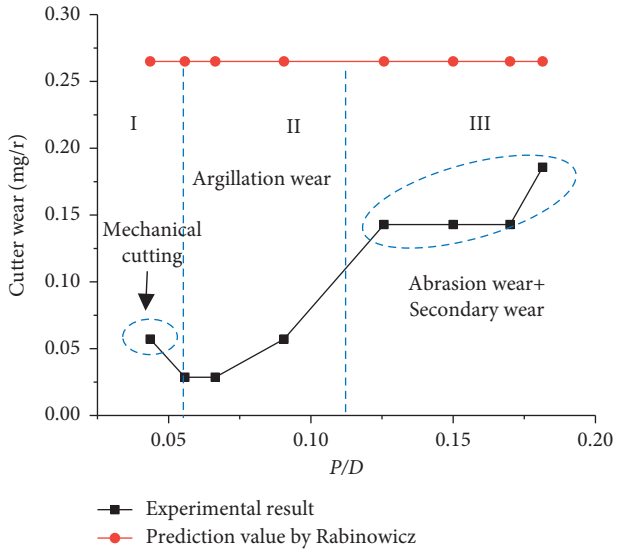

Figure 6: Variation of cutter wear per rotation during the tunnelling process.

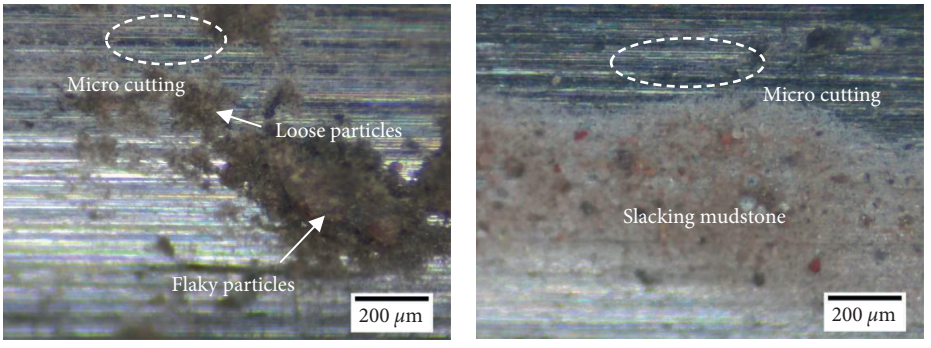

Figure 7: Continued.

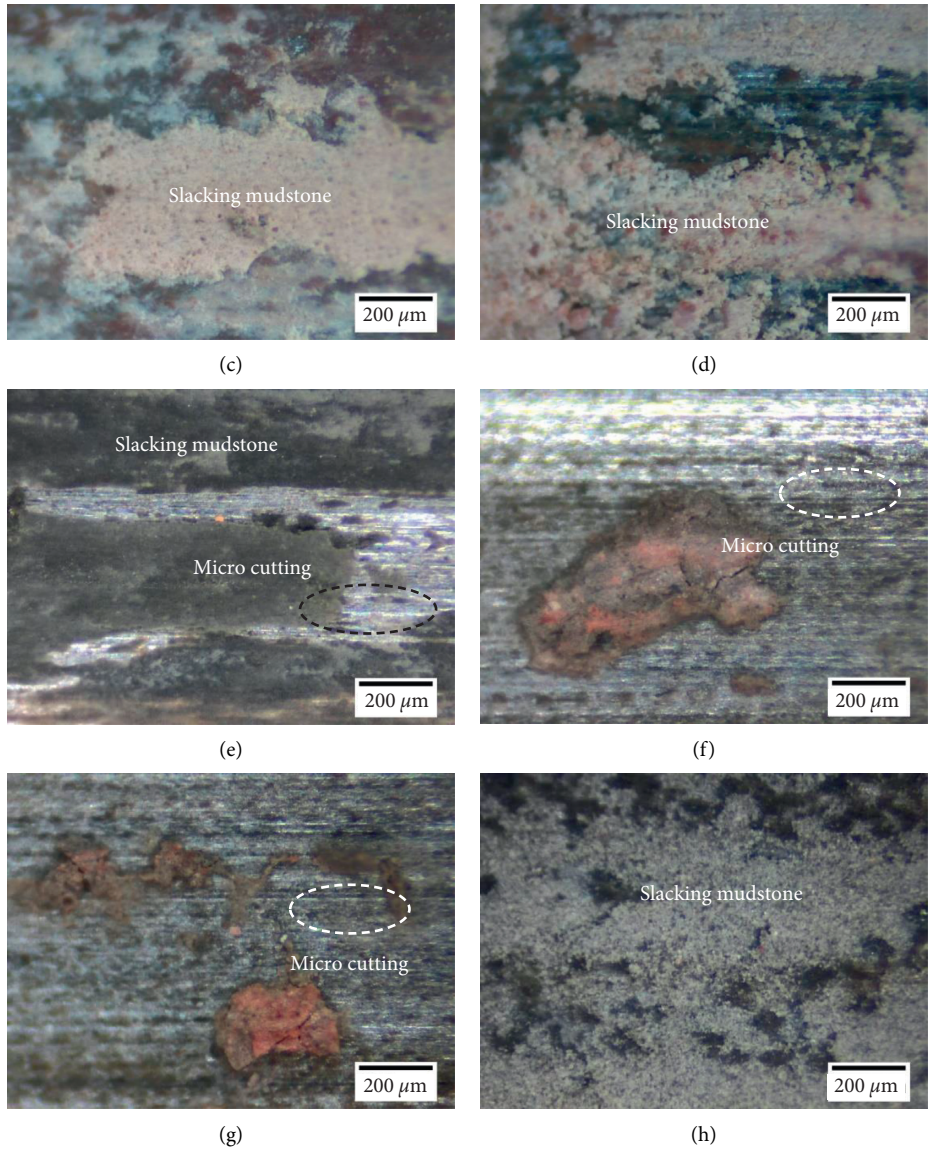

Figure 7: Evolution of disc cutter wear at ×400 magnification. (a) 5 min, $P/D = 0.04$; (b) 10 min, $P/D = 0.06$; (c) 15 min, $P/D = 0.07$; (d) 20 min, $P/D = 0.09$; (e) 30 min, $P/D = 0.13$; (f) 40 min, $P/D = 0.15$; (g) 50 min, $P/D = 0.17$; (h) 60 min, $P/D = 0.18$.

4.1. The Evolution of Argillization by Disc Cutter. According to the distribution of the micropores, slacking mudstone on cutting groove, and the porosity of slacking mudstone, the argillization process of mudstone by disc cutter can be categorized into three stages, namely, the mechanical cutting stage ($P/D < 0.06$), the deterioration of the microstructure and the formation of slaking mudstone stage ($0.06 \le P/D \le 0.09$), and adhesion of slacking mudstone stage ($P/D > 0.09$). The mechanism of each stage is as follows.

4.1.1. Mechanical Cutting Stage ($P/D < 0.06$). Once the disc cutter penetrates into the mudstone, the water added on the cutter reduces the adhesion of the clay on the cutter. The cutter directly contacts with the rock. Therefore, under the normal force and rolling force, microcracks and obvious abrasion mark appear on the cutting groove (Figure 3(a)). Moreover, part of the rock is directly cut into flake particles (Figure 4(a)). Due to the friction between hard mineral particles in rocks and cutters, cutter wear is obvious.

Besides, at this stage, the friction between the cutter and the hard rock particles will generate much friction heat. In order to quantitatively study the friction heat, the variations of the maximum temperature and the difference between the maximum and minimum temperature on the cutter ring were measured, as shown in Figure 8. In this figure, I, II, and III represent the mechanical cutting stage ($P/D < 0.06$), the deterioration of the microstructure and the formation of slaking mudstone stage ($0.06 \le P/D \le 0.09$), and adhesion of slacking mudstone stage ($P/D > 0.09$), respectively. In the mechanical cutting stage, the maximum temperature and temperature difference on the cutter ring increase rapidly. When $P/D = 0.06$, the maximum temperature and

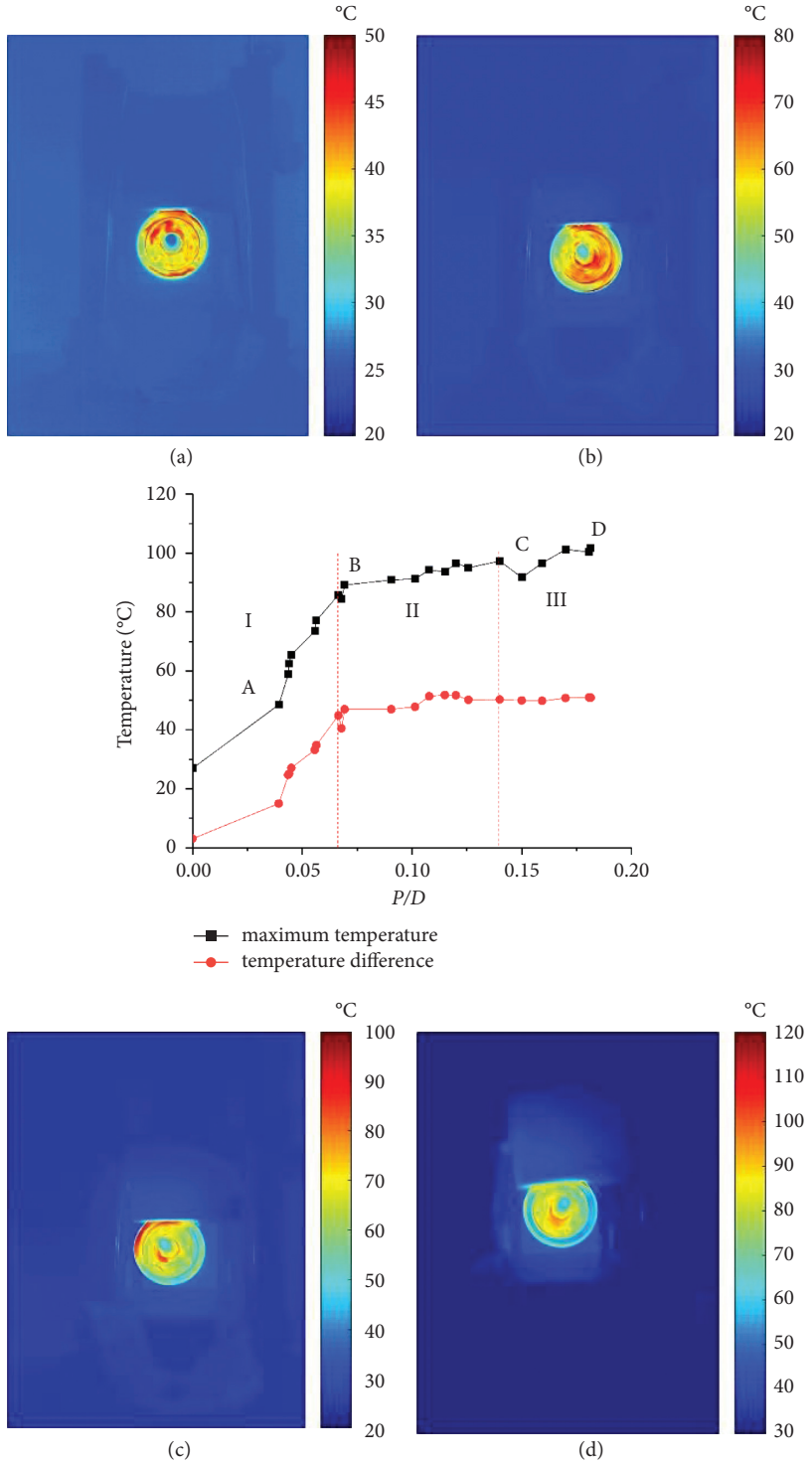

Figure 8: Curves of the maximum temperature and temperature difference on cutter ring.

temperature difference reach 85.8°C and 44.9°C, respectively. After that, the increase rates of both values slow down. The maximum temperature and temperature difference are 101.6°C and 50.9°C, respectively. Correspondingly, in the mechanical cutting stage, it can be seen from the temperature field of the cutter (point A) that the friction between the cutter ring and the rock gives rise to high temperature, and the temperature is significantly greater than the cutter body. The temperature distribution on the cutter ring is relatively uniform, so the temperature difference is small at this stage. After the mechanical cutting stage (points B, C, D), the maximum temperature of the cutter ring gradually increases, but the temperature distribution of the cutter ring is uneven, and high temperature distributes at the contact

area between the rock and cutter ring, causing the temperature difference increases.

Based on the experimental results mentioned above, it is concluded that the temperature on the cutter is determined by the friction heat and water evaporation, as shown in Figure 9. On the one hand, the temperature on the cutter is mainly caused by the friction between the cutter ring and mineral particles in the rock. Under the action of mechanical cutting, the temperature of the cutter ring rises rapidly. Subsequently, due to heat conduction, the temperature on the cutter ring is transferred to the cutter body and the cutter shaft. However, on the other hand, as the water addition and the evaporation of water inside the rock absorb the friction heat, the temperature on cutter ring far away from contact area decreases. Therefore, the temperature distribution on the cutter ring is uneven, resulting in the change of temperature difference. That is to say, the temperature difference on the cutter reflects the relative effect of water evaporation and frictional heat. The more obvious the evaporation, the greater the temperature difference. Finally, friction and water evaporation reach at a dynamic balance condition, and the temperature on the cutter ring keeps stable.

In engineering practice, the cutter rolls on the tunnel surface for a long time, causing the high temperature. In order to enhance the cooling effect of water, an appropriate amount of refrigerant can be added in water. Besides, lubricants can be added to the soil bin and the cutterhead to reduce the friction between the cutter and the rock.

4.1.2. Deterioration of Mudstone and the Formation of Slacking Mudstone Stage ($0.06 \le P/D \le 0.09$). Deterioration of the microstructure of mudstone and formation of slacking mudstone is an important process in the TBM tunnelling, which determines rock breaking efficiency and cutter wear. According to the microstructure of cutting groove, the failure mechanism of microstructure of mudstone under the action of cutter is summarized as follows:

(i) The weakening effect of water promotes the formation of slacking mudstone. Although the microscopic cracks generated in the mechanical cutting stage have little effect on the permeability of mudstone, they increase the free energy of the rock surface and enhance the adsorption of pore water [30]. The water migrates towards the microcracks under the action of adsorption force. Due to the weakening effect of water, uneven expansion of minerals [31, 32], dissolution of cements [33], and destruction of mineral lattices [34, 35] will occur. The bond between the clay minerals and the particle skeleton is deteriorated. The cementation force between them is reduced, causing the clay mineral particles to separate from the skeleton of coarse particles. Eventually, the mudstone disintegrates.

Zhang et al. [36] pointed out that the water absorption and expansion of soft rock can be divided into cementing expansion and internal expansion. Specifically, cementing expansion is caused by the "effect of water film" on the surface of clay minerals, as shown in Figure 10(a). At free state, due to the electrostatic attraction on the surface of clay mineral particles, a strong electrostatic attraction field occurs around the particles. Under the action of electrostatic gravity field, water molecules increasing can be adsorbed around clay particles. Thus the thickness of water film on the surface of clay particles becomes increased. The bond strength between clay mineral particles is weakened. In contrast, cementing expansion typically occurs in the illite, which leads to the expansion of soft rock and reduction of mechanical strength. As shown in Figure 8(b), the crystal lattice of illite consists of a layer of aluminum and two layers of silicon. Besides, an ion layer lies between the crystal lattice of illite. The water molecule particles can infiltrate the counterion layer, causing the escape of ion. Therefore, spacing between the crystal lattice increases. As a result, the clay particles swell gradually. The water absorption and expansion of soft rock will increase the distance between clay particles and weaken the bonding strength of mineral particles. Therefore, in Figures 3(b)–3(d), the slacking mudstone gradually occurs on the cutting grooves. Furthermore, the expansion of slacking mudstone leads to the decrease in porosity of rock cutting groove and the increase in average particle size of slacking mudstone.

(ii) Temperature effect can promote the generation of microcracks through thermal expansion. From the change of cutter temperature, it can be seen that, in the deterioration of mudstone and the formation of slacking mudstone stage, the cutter temperature gradually reaches the maximum value. Therefore, thermal stress distributes inside the rock. When the stress exceeds the tensile strength of the rock, microcracks will appear inside the rock. The coarse particle skeleton-flocculation structure will be destroyed. Furthermore, clay minerals and skeleton particles will be separated. In addition, high temperature can also improve the hydration reaction rate of illite in mudstone, so the formation of slacking mudstone is accelerated further.

(iii) Mechanical movement accelerates the argillization process by mechanical activation. When the microstructure of mudstone deteriorates under the action of water, it is also subjected to the mechanical action of cutter, which is the main difference from mudstone argillization under natural conditions. In the process of argillization by disc cutter, the mechanical action reduces the particle size of mineral particles, increasing its specific surface area and surface energy. Under the action of mechanical activation, the uneven expansion of mineral particles, cement dissolution, and mineral secondary reaction process are accelerated [10]. In addition, mechanical action leads to the redistribution of

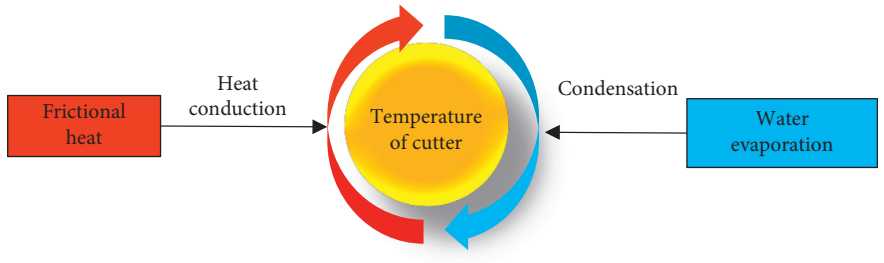

Figure 9: Schematic diagram of the change in disc cutter temperature.

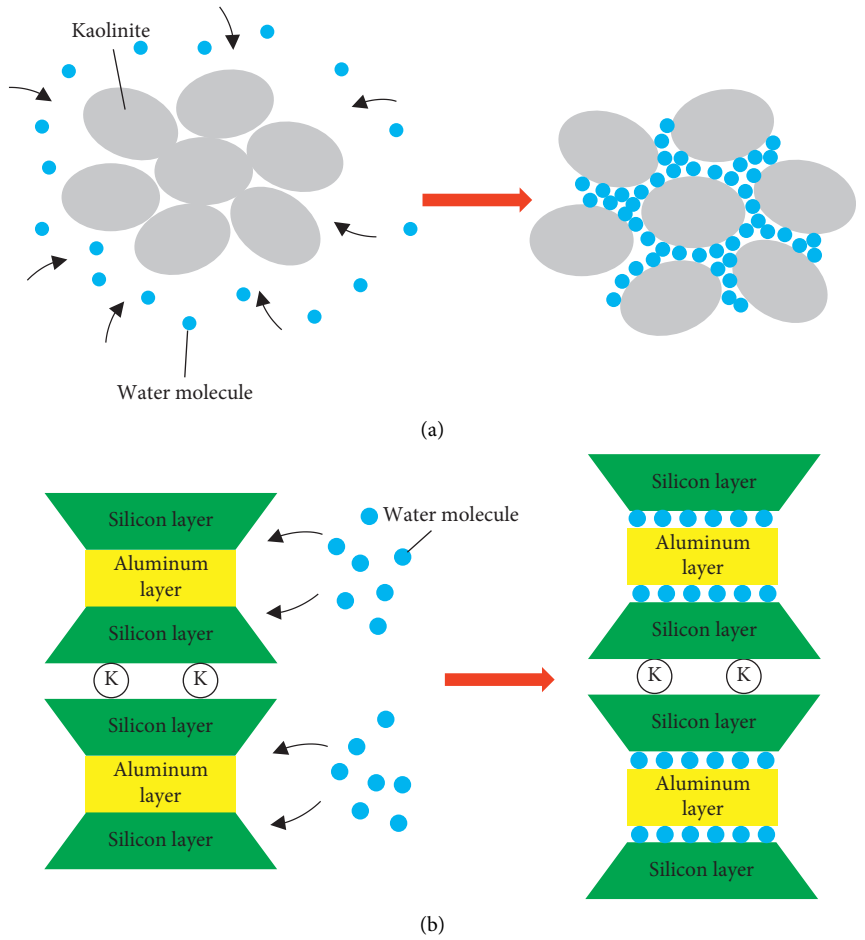

Figure 10: Swell mechanism of the soft rock: (a) cementing expansion; (b) internal expansion.

mineral particles, causing the damage of connection between clay particles and coarse grain skeleton. Mohammadabad et al. [37] found that the mineral structure of chalcopyrite can be redistributed after grinding, so the extraction efficiency is improved. Similarly, the redistribution of minerals in mudstone in the test improves the activity of minerals, which is conducive to the argillization effect.

4.1.3. Adherence of Slacking Mudstone Stage (P/D > 0.09). With the indentation of the cutter, the cementation force between the clay particles and the coarse grain skeleton decreases. Finally, the clay particles are taken away from the rock. Therefore, micropores and micropits occur on the cutting groove, and the porosity of the cutting groove surface increases. After the formation of slacking mudstone, the particle size decreases under the action of the cutter. Due to the abrasive wear, microcutting and furrow occur on the disc cutter. Thus some slacking mudstone will be filled into microcutting and furrow during the tunnelling. Eventually, some slacking mudstone will be adhered to the surface of the cutter, as shown in Figure 11. Furthermore, under the friction between disc cutter and the rock, the internal shear failure of the slacking mudstone occurs simultaneously [38]. This will further reduce the free energy of clay minerals,

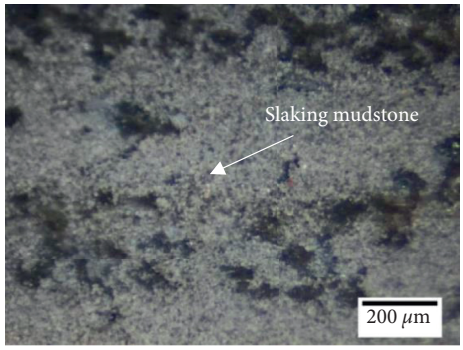

Figure 11: Slaking mudstone adhered to disc cutter.

causing the recrystallization and aggregation of crystal particles. Under the high temperature and high pressure, the hammer welding inside the mineral crystal will result in the formation of slacking mudstone with high viscosity and high density. Thus the "mud cake" is formed.

4.2. The Cutter Wear Mechanism considering the Argillation Effect. In Section 3.2, it is seen that the microstructures of the mudstone and worn surface of the disc cutter exert various characteristics during the tunnelling process. Therefore, on consideration of the argillization, it can be speculated that the wear mechanism of disc cutter differs in each stage. According to the distribution of microcutting and the slacking mudstone, the evolution of cutter wear considering the argillation effect can be divided into three stages: mechanical wear stage ($P/D < 0.06$), argillization wear stage ($0.06 \le P/D < 0.13$), and secondary wear stage ($P/D \ge 0.13$). The cutter wear mechanism at each stage is as follows:

(i) Mechanical wear stage ($P/D < 0.06$): at the mechanical wear stage, abrasive wear is the main reason for the wear loss of disc cutter. In Figure 7(a), obvious microcutting can be seen on the surface of cutter. Only some loose particles and flaky particles occur. This indicates that the slacking mudstone is not formed at this stage. Under the normal force, hard particles in the rock block pierce into the cutter. Then the steel is removed with the rolling of cutter, leaving the microcutting on the cutter surface [39].

(ii) Argillization wear stage ($0.06 \le P/D < 0.13$): at argillization wear stage, the slacking mudstone between the disc cutter and the hard mineral particles inside the mudstone reduces the wear rate of the disc cutter. With the penetration of disc cutter, the slacking mudstone is formed gradually due to the water-weakening effect. Consequently, some slacking mudstone is filled into the microcutting (Figures 7(b)–7(d). As the slacking mudstone uniformly distributes on the cutter surface, the hard particles in rock block and cutter are separated. The "separation effect" decreases the wear rate (Figure 6).

(iii) Secondary wear stage ($P/D \ge 0.13$): during the TBM tunnelling, if the rock chips are not carried out in time, the friction between rock chips and cutter will cause the wear of cutter body. This kind of wear form is defined as the secondary wear. The secondary wear increases the wear loss of disc cutter. In the mudstone layer, with the formation of the slacking mudstone, the secondary wear appears, so the wear rate increases gradually (Figure 6). As the test proceeds, the temperature on cutter ring exceeds 90 deg after P/D of 0.13 (Figure 8). In the experiment, it is observed that the slacking mudstone adhered to cutter ring shrinks due to the water evaporation. Consequently, the stickiness of the slacking mudstone is reduced. The slacking mudstone on cutter surface disappears gradually (Figures 7(e)–7(g)). Due to the weakening of "separation effect," wear rate increases dramatically. Finally, with the rolling of disc cutter, mechanical effect, temperature, and the stickiness of the slacking mudstone reach dynamic balance condition. All of these factors determine the mass of slacking mudstone adhered to cutter ring. At this moment, the slacking mudstone distributes on the cutter uniformly (Figure 7(h)). On the other hand, after P/D of 0.13, penetration depth exceeds 9.1 mm in this experiment, the cutter ring is caught in rock block thoroughly, causing the wear of cutter body, and the secondary wear occurs. The combined effects of abrasion wear and secondary wear increase cutter wear under the condition of argillization. During the tunnelling of TBM in mudstone, when the cutterhead is clogged, the friction between cutter body and rock chips will lead to the secondary wear. Therefore, measures are necessary to be taken to prevent the clogging problems.

When TBMs excavate in hard rock, the main mechanism of disc cutter is abrasive wear, which is similar to that in mechanical wear stage [22]. By comparison, it is found that the cutter goes through mechanical wear stage, argillization wear stage, and secondary wear stage when considering the argillization. To compare the cutter wear under the condition of argillization and without argillization, a prediction model proposed by Rabinowicz [40] is employed to calculate the wear loss. In this model, it is believed that the main reason for cutter wear is abrasive wear. The wear loss is obtained by

$$V = K_s \frac{F_n L}{H}, \tag{1}$$

where V is the volume of cutter wear, K_S represents coefficient of abrasive wear, F_n stands for normal force, L is the sliding distance of the hard particles, and H is the hardness of the steel. In this study, $K_S = 1.5 \times 10^{-3}$, $F_n = 150$ N, and the hardness of the H13 steel is 1.949 GPa.

According to equation (1), the abrasion wear without argillization is 0.26 mg/r. The calculated result is plotted in Figure 6. By comparison, it is seen that the abrasion wear without argillization is much larger that under the condition of argillization. The main reason for this phenomenon is that

the slacking mudstone and water act as separating agent and lubricant, respectively. Therefore, coefficient of abrasive wear decreases significantly.

4.3. The Relationship between the Evolution of Argillization of Mudstone and Cutter Wear. By comparing the evolution of argillization of mudstone and cutter wear, it is found the mechanical cutting stage and the deterioration of mudstone and the formation of slacking mudstone stage basically correspond to the mechanical wear stage, argillization wear stage, and secondary wear stage, respectively. At the initial stage of TBM tunnelling, effect of mechanical cutting is obvious. Correspondingly, under the action of normal and rolling force, abrasion wear occurs. Subsequently, with the degree of argillization increasing, the slacking mudstone is formed, and thus the wear rate slows down. When the mechanical effect, temperature, and the stickiness of the slacking mudstone reach dynamic balance condition, the stickiness of the slacking mudstone is reduced, causing the increase in the cutter wear rate.

5. Conclusions

The argillization is frequently encountered during the excavation of TBM in the mudstone, which leads to the clogging of the TBM cutterhead. To investigate the evolution of argillization of mudstone and cutter wear during the TBM tunnelling, a series of rotary indentation tests were carried out on the self-design experimental bench. Subsequently, according to the microstructures of cutting grooves and worn surface of disc cutter, mechanisms of argillization and cutter wear are revealed. The main conclusions can be drawn as follows:

The argillization process of mudstone by disc cutter is divided into three stages: the deterioration of mudstone and the formation of slacking mudstone stage and the adherence of slacking mudstone stage. At the mechanical cutting stage, the rock is broken mainly by the cutting force. The temperature on the cutter ring increases rapidly. Subsequently, at mudstone microstructure degradation and argillaceous formation stage, the weakening effect of water, temperature effect, and mechanical activation cause the microstructure damage of mudstone and formation of slacking mudstone. Finally, at the adherence of slacking mudstone stage, the slacking mudstone is adhered to the cutter surface under the normal force. The recrystallization of the crystal particles will eventually lead to the "mud cake" of the cutterhead.

Correspondingly, the wear process of disc cutter under the condition of the argillization is categorized into the mechanical wear stage, argillization wear stage, and secondary wear stage. At mechanical wear stage, cutter wear is mainly caused by abrasion wear. Subsequently, the formation of slacking mudstone decreases the wear rate due to the "separation effect." Finally, cutter wear increases by the combined effects of abrasion wear and secondary wear. The evolution of cutter wear corresponds to the evolution of the argillization process of mudstone.

Data Availability

All data, models, and code generated or used during the study appear in the published article.

Conflicts of Interest

The authors declare no conflicts of interest, including specific financial interests and relationships relevant to subject of this paper.

Acknowledgments

The financial support from the Graduate Research and Innovation Foundation of Chongqing, China (Grant no. CYB21032), and the Natural Science Fund of China (Grant no. 51879016) is greatly appreciated.

References

[1] Y. J. Bao, J. L. Chen, and B. S. Jiang, "Breakage mechanism of layered sandstone penetrated by TBM disc cutter," *Shock and Vibration*, vol. 2021, Article ID 6618234, 17 pages, 2021.

[2] M. Heuser, G. Spagnoli, P. Leroy, N. Klitzsch, and H. Stanjek, "Electro-osmotic flow in clays and its potential for reducing clogging in mechanical tunnel driving," *Bulletin of Engineering Geology and the Environment*, vol. 71, no. 4, pp. 721–733, 2012.

[3] S. Qiao, Y. M. Xia, Z. Z. Liu, J. S. Liu, B. Ning, and A. L. Wang, "Performance evaluation of bolter miner cutting head by using multicriteria decision-making approaches," *Journal of Advanced Mechanical Design, Systems, and Manufacturing*, vol. 11, no. 5, pp. 17–00273, 2017.

[4] C. Oggeri, T. M. Fenoglio, and R. Vinai, "Tunnel spoil classification and applicability of lime addition in weak formations for muck reuse," *Tunnelling and Underground Space Technology*, vol. 44, no. 3, pp. 97–107, 2014.

[5] A. Bruland, *Hard rock tunnel boring*, Ph.D. Thesis, Norwegian University of Science and Technology, Trondheim, Norway, 1998.

[6] N. Barton, *TBM Tunneling in Jointed and Fault Rock*, Balkema, Rotterdam, Netherlands, 2000.

[7] X. Liu, M. Xu, and P. Qin, "Joints and confining stress influencing on rock fragmentation with double disc cutters in the mixed ground," *Tunnelling and Underground Space Technology*, vol. 83, pp. 461–474, 2019.

[8] H. Bejari and J. Khademi Hamidi, "Simultaneous effects of joint spacing and orientation on TBM cutting efficiency in jointed rock masses," *Rock Mechanics and Rock Engineering*, vol. 46, no. 4, pp. 897–907, 2013.

[9] Y. Peng, H. Liu, C. Li, X. Ding, X. Deng, and C. Wang, "The detailed particle breakage around the pile in coral sand," *Acta Geotechnica*, vol. 16, no. 6, pp. 1971–1981, 2021.

[10] Y. Zhou, D. J. Zhao, B. Li, H. Y. Wang, Q. Q. Tang, and Z. Z. Zhang, "Fatigue damage mechanism and deformation behaviour of granite under ultrahigh-frequency cyclic loading conditions," *Rock Mechanics And Rock Engineering*, vol. 54, 2021.

[11] J. T. Yi, F. Liu, T. B. Zhang, K. Yao, and G. Zhen, "A large deformation finite element investigation of pile group

installations with consideration of intervening consolidation," *Applied Ocean Research*, vol. 112, Article ID 102698, 2021.

[12] Q. M. Gong, Y. Y. Jiao, and J. Zhao, "Numerical modelling of the effects of joint spacing on rock fragmentation by TBM cutters," *Tunnelling and Underground Space Technology*, vol. 21, no. 1, pp. 46–55, 2006.

[13] B. Liu, H. Yang, E. Haque, and G. Wang, "Effect of joint orientation on the breakage behavior of jointed rock mass loaded by disc cutters," *Rock Mechanics and Rock Engineering*, vol. 54, no. 4, pp. 2087–2108, 2021.

[14] Q. M. Gong, Q. R. She, and J. M. Wang, "Influence of different thicknesses of marble layers on TBM excavation," *Chinese Journal of Rock Mechanics and Engineering*, vol. 29, no. 7, pp. 1442–1449, 2010.

[15] H. Ma, L. Yin, Q. Gong, and J. Wang, "TBM tunneling in mixed-face ground: problems and solutions," *International Journal of Mining Science and Technology*, vol. 25, no. 4, pp. 641–647, 2015.

[16] D.-J. Ren, S.-L. Shen, A. Arulrajah, and W.-C. Cheng, "Prediction model of TBM disc cutter wear during tunnelling in heterogeneous ground," *Rock Mechanics and Rock Engineering*, vol. 51, no. 11, pp. 3599–3611, 2018.

[17] J. Zhao, Q. M. Gong, and Z. Eisensten, "Tunnelling through a frequently changing and mixed ground: a case history in Singapore," *Tunnelling and Underground Space Technology*, vol. 22, no. 4, pp. 388–400, 2007.

[18] H. Yang, B. Liu, Y. Wang, and C. Li, "Prediction model for normal and flat wear of disc cutters during TBM tunneling process," *International Journal of Geomechanics*, vol. 21, no. 3, Article ID 06021002, 2021.

[19] A. Lislerud, *Principles of Mechanical Excavation*, Possiva report, Helsinki, 1997.

[20] N. Espallargas, P. D. Jakobsen, L. Langmaack, and F. J. Macias, "Influence of corrosion on the abrasion of cutter steels used in TBM tunnelling," *Rock Mechanics and Rock Engineering*, vol. 48, no. 1, pp. 261–275, 2015.

[21] M. Petrica, E. Badisch, and T. Peinsitt, "Abrasive wear mechanisms and their relation to rock properties," *Wear*, vol. 308, no. 1-2, pp. 86–94, 2013.

[22] M. Petrica, M. Painsi, E. Badisch, and T. Peinsitt, "Wear mechanisms on martensitic steels generated by different rock types in two-body conditions," *Tribology Letters*, vol. 53, no. 3, pp. 607–616, 2014.

[23] J. Rostami, A. Ghasemi, E. Alavi Gharahbagh, C. Dogruoz, and F. Dahl, "Study of dominant factors affecting cerchar abrasivity index," *Rock Mechanics and Rock Engineering*, vol. 47, no. 5, pp. 1905–1919, 2014.

[24] C. Frenzel, H. Käsling, and K. Thuro, "Factors influencing disc cutter wear," *Geomechanik und Tunnelbau*, vol. 1, no. 1, pp. 55–60, 2008.

[25] T. N. Michalakopoulos, V. G. Anagnostou, M. E. Bassanou, and G. N. Panagiotou, "The influence of steel styli hardness on the Cerchar abrasiveness index value," *International Journal of Rock Mechanics and Mining Sciences*, vol. 43, no. 2, pp. 321–327, 2006.

[26] F. J. Macias, F. Dahl, and A. Bruland, "New rock abrasivity test method for tool life assessments on hard rock tunnel boring: the Rolling Indentation Abrasion Test (RIAT)," *Rock Mechanics and Rock Engineering*, vol. 49, no. 5, pp. 1679–1693, 2016.

[27] X. Zhang, Y. Xia, Y. Zhang, Q. Tan, Z. Zhu, and L. Lin, "Experimental study on wear behaviors of TBM disc cutter ring under drying, water and seawater conditions," *Wear*, vol. 392-393, pp. 109–117, 2017.

[28] B. Liu, H. Yang, and S. Karekal, "Reliability analysis of TBM disc cutters under different conditions," *Underground Space*, vol. 6, no. 2, pp. 142–152, 2021.

[29] K. L. Johnson, *Contact Mechanics*, Cambridge University Press, Nineth printing, Cambridge, UK, 2003.

[30] H. W. Huang and P. Che, "Research on micro-mechanism of softening and argillitization of mudstone," *Journal of Tongji University*, vol. 35, no. 7, pp. 866–870, 2007, in Chinese.

[31] B. C. Hawlader, Y. N. Lee, and K. Y. Lo, "Three-dimensional stress effects on time-dependent swelling behaviour of shaly rocks," *Canadian Geotechnical Journal*, vol. 40, no. 3, pp. 501–511, 2003.

[32] C. L. Zhang, K. Wieczorek, and M. L. Xie, "Swelling experiments on mudstones," *Journal of Rock Mechanics and Geotechnical Engineering*, vol. 2, pp. 44–51, 2010.

[33] J. C. Dick and A. Shakoor, "Lithological controls of mudrock durability," *The Quarterly Journal of Engineering Geology and Hydrogeology*, vol. 25, no. 1, pp. 31–46, 1992.

[34] Q. Jiang, J. Cui, X. Feng, and Y. Jiang, "Application of computerized tomographic scanning to the study of water-induced weakening of mudstone," *Bulletin of Engineering Geology and the Environment*, vol. 73, no. 4, pp. 1293–1301, 2014.

[35] R. Doostmohammadi, M. Moosavi, T. Mutschler, and C. Osan, "Influence of cyclic wetting and drying on swelling behavior of mudstone in south west of Iran," *Environmental Geology*, vol. 58, no. 5, pp. 999–1009, 2009.

[36] S. Zhang, Q. Xu, and Z. Hu, "Effects of rainwater softening on red mudstone of deep-seated landslide, Southwest China," *Engineering Geology*, vol. 204, pp. 1–13, 2016.

[37] F. K. Mohammadabad, S. Hejazi, J. V. Khaki, and A. Babakhani, "Mechanochemical leaching of chalcopyrite concentrate by sulfuric acid," *International Journal of Minerals, Metallurgy, and Materials*, vol. 23, no. 4, pp. 380–388, 2016.

[38] Y. Tsubakihara, H. Kishida, and T. Nishiyama, "Friction between cohesive soils and steel," *Soils and Foundations*, vol. 33, no. 2, pp. 145–156, 1993.

[39] L. Lin, Q. Mao, Y. Xia et al., "Experimental study of specific matching characteristics of tunnel boring machine cutter ring properties and rock," *Wear*, vol. 378-379, pp. 1–10, 2017.

[40] E. Rabinowicz, "Friction and wear of materials," *Wear*, vol. 8, no. 6, p. 491, 1965.